Hyperspectral Image Reconstruction of Heritage Artwork Using RGB Images and Deep Neural Networks

Ailin Chen
Departamento de Conservação e Restauro and NOVA LINCS, Faculdade de Ciências e Tecnologia, Universidade NOVA de Lisboa
Monte da Caparica, Caparica
Portugal
ailin.chen@campus.fct.unl.pt

Rui Jesus
NOVA-LINCS, NOVA School of Science and Technology
Monte da Caparica, Portugal, Instituto Superior de Engenharia de Lisboa/IPL
Lisboa, Portugal
rjesus@deetc.isel.ipl.pt

Márcia Vilarigues
Department of Conservation and Restoration & VICARTE, NOVA School of Science and Technology
Monte da Caparica, Caparica
Portugal
mgv@fct.unl.pt

ABSTRACT

The application of our research is in the art world where the scarcity of available analytical data from a particular artist or physical access for its acquisition is restricted. This poses a fundamental problem for the purpose of conservation, restoration or authentication of historical artworks. We address part of this problem by providing a practical method to generate hyperspectral data from readily available RGB imagery of artwork by means of a two-step process using deep neural networks. The particularities of our approach include the generation of learnable colour mixtures and reflectances from a reduced collection of prior data for the mapping and reconstruction of hyperspectral features on new images. Further analysis and correction of the prediction are achieved by a second network that reduces the error by producing results akin to those obtained by a hyperspectral camera. Our method has been used to study a collection of paintings by Amadeo de Souza-Cardoso where successful results were obtained.

CCS CONCEPTS

• **Computing methodologies** → **Neural networks**; **Artificial intelligence**; • **Applied computing** → **Arts and humanities**.

KEYWORDS

Neural Networks, Hyperspectral Imaging, Image Visualisation, Colour Analysis

ACM Reference Format:
Ailin Chen, Rui Jesus, and Márcia Vilarigues. 2022. Hyperspectral Image Reconstruction of Heritage Artwork Using RGB Images and Deep Neural Networks. In *International Conference on Content-based Multimedia Indexing (CBMI 2022), September 14–16, 2022, Graz, Austria.* ACM, New York, NY, USA, 6 pages. https://doi.org/10.1145/3549555.3549583

CBMI 2022, September 14–16, 2022, Graz, Austria

ACM ISBN 978-1-4503-9720-9/22/09…$15.00
https://doi.org/10.1145/3549555.3549583

1 INTRODUCTION

The technique of hyperspectral imaging has been employed extensively in multitudinous fields, ranging from the more widely-applied territories such as geoscience and agriculture to the more recent applications like in cultural heritage and the art arena. This is due to its particular capability to reveal a specific series of hidden features that other technologies may not be able to uncover. These hidden features can be useful for the purpose of conservation or authentication of artworks [8] or even in image retrieval systems [5] in other contexts. Nevertheless, in the art world, in particular, the difficulty to perform analysis of cultural and historical artworks intensifies as the number of artworks for any given artist is limited and access to original items for data acquisition can be unattainable. It is thus significant and useful to devise methods to estimate certain data, for example, hyperspectral images from existing accessible information, typically from RGB images.

One of the more recent analysis tools that have become increasingly significant in various genres of studies over the past few years is the state-of-the-art technique of Deep Neural Networks (DNNs) given their suitability to analyse data, recognise and classify patterns with their brain style processing. Although the concept and approach of DNNs are being used extensively in other scientific fields, their application in the art world is still reduced. Our study aims therefore to develop practical methods applying DNNs in the reconstruction of hyperspectral images from RGB images of paintings. More specifically, we focus on the particular case where a limited but incomplete set of hyperspectral data from basic oil pigments used by an artist is available. The case study evaluated in our research focuses on the paintings of the late Portuguese artist Amadeo de Souza-Cardoso whose collection of pigment data and hyperspectral images are available at the Universidade Nova the Lisboa. While the method and results are focused on this particular artist due to the availability of data, the methods can be generalised and be applied to other artists and pigment media such as pencil drawings or watercolour paintings.

Earlier studies dealing with RGB image conversion to reflectances have existed for a while, initially from a physics point of view, in other words, without the involvement of machine learning algorithms. Typical examples include [12] where a spectrally-based renderer was created in an optimal metamer space to produce physically-plausible spectra, or [1] where an easy, flexible and repetitive physical rendering approach was designed for the conversion from the RGB image to spectral information. Another physical approach for spectral reconstruction includes the manipulation of digital cameras and exploitation of the properties of those camera sensors, like the work done in [9] and [4]. Mathematical approaches include for example [3] where a sparse dictionary of hyperspectral signatures was derived from a collection of known hyperspectral data in order to recover hyperspectral information for novel RGB images.

In recent years, research using machine learning techniques to reconstruct hyperspectral signals has also been studied. For example, [2] intended to recover hyperspectral data from the RGB image of the same object by applying a Gaussian process under a full Bayesian model, and by training a set of known spectral information of other objects. Regarding the use of neural networks, the study has focused on approaches like [10] where two advanced Convolutional Neural Networks (CNNs) coined as HSCNN-R and HSCNN-D were introduced and analysed, with the latter built upon the former. [10] proposed the HSCNN model to recover hyperspectral data from a single super-resolution RGB image with HSCNN-R based on DNNs and a series of residual blocks, while HSCNN-D deepens the network by replacing the residual blocks in HSCNN-R with dense blocks accompanied by a novel fusion scheme. Other approaches included [13] where a U-net based structure named C2H-Net showed promising results of the spectral information obtained because they have addressed some of the limitations of current CNN techniques. [6] experimented with both 2D and 3D CNNs architectures where the former focused on spatial correlation and the latter on inter-channel correlation. Another example where a robust HSCNN-R trained based on the mean relative absolute error loss function (MRAELF) was developed by [14] where it was deemed that this function was preferred when all wavelengths were considered equally important. While all these CNN-based methods are promising, the nature of their implementation in a practical framework can be computationally expensive and, in many cases, requires a large training dataset to achieve the reported results. Furthermore, these focused on their application from a distinct point of view based on the data accessible locally.

Our work reported in this paper is a by-product of our primary interest and differs from other methods by providing an approach that uses a significantly reduced training set and architecture based on two DNNs with one reconstructing the hyperspectral image while the other corrects for biases from the acquisition method. In particular, our research is centred on the specific art world, where such work is still comparably scarce.

2 PROBLEM FORMULATION

As mentioned previously, hyperspectral imaging is particularly important for applications related to the analysis and visualisation of artworks as it provides researchers with powerful information related to the colour content of the object of study. This hyperspectral data is typically obtained using suitable hyperspectral cameras that, although they are non-invasive, require access to original artwork which can be not only challenging but also expensive. To overcome this, we focus on a method that allows the estimation of hyperspectral data from RGB images based on the use of prior and exemplary data. More specifically, the objective of this research is to estimate the hyperspectral image $\bar{\mathbf{Z}} \in \mathbb{R}^{W \times H \times B}$ where W, H and B are the width, height and number of spectral bands respectively, for the RGB image of the same painting $\mathbf{I} \in \mathbb{R}^{W \times H \times 3}$. For the reconstruction of $\bar{\mathbf{Z}}$, two sets of reference data are available. First, a collection of N base pigment colours $\mathbf{P}_i, i \in \{1...N\}$ with associated reflectance values P_λ known to have been used in at least one painting of the same collection. The second set of data includes an exemplary group of hyperspectral signatures $\mathbf{S} \in \mathbb{R}^B$ from a painting obtained with a hyperspectral camera. While the problem described can be applied to multiple fields, our research focuses particularly on the specific application to artworks, namely paintings.

3 METHOD PROPOSED

The method we propose is a practical approach with low computation cost consisting of a 2-step process where two Deep Neural Networks are used to estimate the hyperspectral image from an RGB image of heritage artwork (Fig. 1). First, an initial hyperspectral estimate is obtained by pixel-wise evaluation of the colour components of a given artwork RGB image with a DNN pretrained with a plurality of reflectances generated from a base set of data known to have been used in artwork from the same artist. The acquisition method, equipment, conditions and number of base pigments can differ from those in the artwork analysed. Consequently, the initial hyperspectral approximation presents an error when compared to data obtained with a given hyperspectral camera. We correct for these effects through the use of a second network trained with predicted and true hyperspectral data thus resulting in a hyperspectral image that closely resembles the output of the hyperspectral camera. We first describe the networks and data pre-processing used and then present the results obtained with the method proposed.

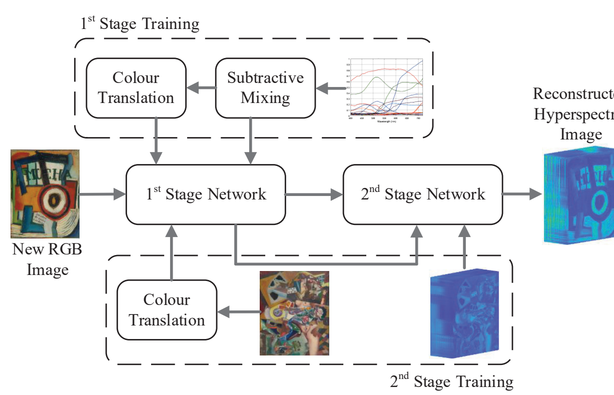

Figure 1: Block diagram of the model proposed. The first stage network is trained with a set of colour components and artificially generated reflectances. The second stage network is trained with the predicted reflectances of the first stage for a given set of colours and true reflectances. ©Center of Modern Art of Calouste Gulbenkian Foundation, Lisbon.

3.1 Colour to Hyperspectral Conversion

The initial hyperspectral estimate is attained through the use of a DNN where the colour parameters to reflectance relationship are learned. This learning process requires a large number of training samples in order to produce an effective reflectance estimate. Given a limited number of base pigments and their associated reflectance known to have been used by a particular artist, a new expanded dataset can be generated by applying colour mixing theory. This is based on synthesising new colours by mixing the reflectances of two or more pigments, a practice widely used by artists in their artwork. Contrary to the colour mixing theory of lights where the superimposition of colours is typically of additive nature the mixing of colours in paintings is subtractive. This is, the combination of two or more pigments do not yield white. In this work, we propose the use of a pure subtractive mixing approach as defined in Eq. 1 [11] where c_i is the proportion of the i^{th} pigment colour and with the sum of all proportions equal to 1. Other subtractive mixing models like the Kubelka-Munk model [7] can be used if parameters like the absorption and backscattering coefficients of the base pigments are known.

$$P_\lambda = \prod_{i=1}^{n} P_{i,\lambda}^{c_i} \quad (1)$$

The effect of applying Eq. 1 on two pigment reflectances (Cerulean Blue and Yellow Ochre) is observed in Fig. 2. The subtractive nature of the model used generates non-linearly spaced reflectances where lower amplitudes dominate the combined mixture reflectance.

The corresponding CIELab and colour components for each generated mixture are then calculated using the CIE 1931 colour matching functions and using the D65 illuminant. For this first stage network, the CIELab components are the input data and amplitude of the artificial mixture reflectances correspond to the output data.

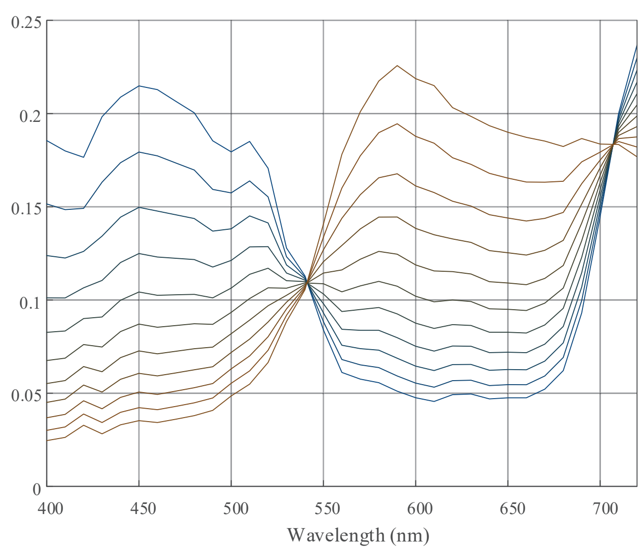

Figure 2: Effect of subtractive mixing of two pigment reflectances using Eq. 1 in steps of 10%.

The neural network proposed is a 7-layer deep feed-forward, fully-connected network with 33, 35, 33, 30, 27, 25 and 20 neurons in each hidden layer respectively and a linear activation function. The training is performed by computing the mean squared error of the targets. New unseen RGB paintings are analysed with the trained network on a pixel-wise basis producing a first approximation of the hyperspectral image based on a set of known pigment reflectances.

3.2 World-Bias Correction

In the second stage of the method proposed, the initial hyperspectral image predicted is evaluated through a second neural network that minimises the error due to the intrinsic nature of the data acquisition process through a given hyperspectral camera. To achieve this, the second stage network is trained with a collection of estimated reflectances from the first network and the corresponding true reflectances extracted from a ground truth RGB and hyperspectral image. This is, the input to this network is the reflectance amplitude of a given pixel estimated by the first network while the output is the 33-point, world-bias corrected reflectance amplitude. The network proposed is a 4-layer deep feed-forward, fully-connected network with 33, 35, 35 and 33 neurons on each hidden layer respectively and with a linear activation function. The correction applied by this network is less complex than the initial colour to reflectance estimation which allows for a lower number of hidden layers required. The performance of the network is computed using the mean square error function.

4 EXPERIMENTAL RESULTS

4.1 Artificial Colour Mixtures

For this work, we use data previously collected by the Department of Conservation and Restoration of the Universidade Nova de Lisboa from the collection of artworks done by Souza-Cardoso. The data contains a database of reflectances from 17 oil pigments acquired using a variety of hyperspectral cameras and known to have been used by Souza-Cardoso. These pigments include Vermilion, Carmine, Raw Sienna, Terra Rosa, Cadmium Orange, Ochre Yellow, Chrome Yellow, Cobalt Violet, Cerulean Blue, Cobalt Blue, Prussian Blue, Cadmium Green, Viridian, Ultramarine, Emerald, Black and Lead White. Artificial mixtures using 3 out of the 17 pigments in steps of 10% were generated using the subtractive mixing model in 1 yielding a total of 44880 mixtures. The respective CIELab colour components for each mixture were also computed.

4.2 Input Data

The data used for evaluation consisted of hyperspectral images of 11 paintings from the collection of Souza-Cardoso with a spectral resolution of 400 nm to 720nm in steps of 10nm acquired with a hyperspectral camera in a previous project by the Department of Conservation and Restoration of the Universidade Nova de Lisboa. For the evaluation, RGB images were generated from the available hyperspectral data applying the D65 illuminant and used as input data for the method proposed. Fig. 3 shows the RGB representation of the selected paintings used through this research for which hyperspectral images were acquired.

Figure 3: RGB representation of the hyperspectral images used. ©Center of Modern Art of Calouste Gulbenkian Foundation, Lisbon.

4.3 Error Measurement

To evaluate the performance of the hyperspectral reconstruction $\bar{\mathbf{Z}}$ with respect to the ground truth $\mathbf{Z}$ we employ the use of Mean Relative Absolute Error (MRAE) defined in Eq. 2 over the Root Square Mean Error as a more suitable metric since this is scale-independent allowing an easier comparison to other methods. A second metric function we use is the Spectral Angle Mapper (SAM) defined in Eq. 3 which computes the angle between the estimated reflectance $\hat{z}_{ij}$ and the ground truth reflectance z_{ij}, averaged over all pixels of the image.

$$MRAE = \frac{1}{n}\sum_{i=1}^{n}\frac{\mid \hat{z}_{ij} - z_{ij} \mid}{z_{ij}} \tag{2}$$

$$SAM = \frac{1}{n}\sum_{i=1}^{n}\cos^{-1}\frac{\hat{z}_{ij}^{T} z_{ij}}{\|\hat{z}_{ij}\|_2 \|z_{ij}\|_2} \tag{3}$$

4.4 Reconstructed Hyperspectral Data

Each of the 11 hyperspectral images in the dataset was converted to RGB and CIELab colour components which then were fed through the 2-stage process to estimate the hyperspectral cube. An example of a reconstructed reflectance obtained for a point of image 86P21 is shown in Fig. 4 along with the ground truth version for comparison. As observed, the overall signature of the reconstructed reflectance shows a similar pattern as that of its ground truth version.

The overall quantitative results of the comparison between original and reconstructed hyperspectral images are shown in Table 1 where the total MRAE and SAM values for each image are presented.

In addition, to aid visual comparison of the results, hyperspectral images at selected wavelengths are displayed in Fig. 6 for painting exhibit 86P21; hyperspectral images are displayed in 8-bit greyscale for visualisation. The error map between the ground truth and the reconstruction highlights the regions where the largest discrepancy is found for the wavelengths selected which appear higher towards the upper end of the spectrum. Finally, a comparison of the RGB images generated from the original and reconstructed hyperspectral images is shown in Fig. 5 with the colour difference measured as the Euclidean distance of the CIELab colour vectors for each pixel.

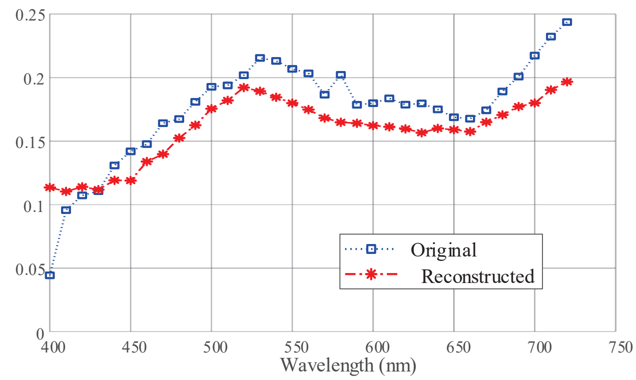

Figure 4: Comparison of ground truth and reconstructed reflectances for pixel 50,50 in painting 86P21.

Table 1: Reconstruction error measured using MRAE and SAM.

Image	MRAE	SAM
68P11	0.0750	0.0815
77P2	0.1384	0.1737
77P5	0.1239	0.0929
77P8	0.1649	0.1473
77P9	0.1755	0.1603
77P16	0.4938	0.1220
77P20	0.9959	0.1155
86P19	0.2524	0.1293
86P21	0.2763	0.1670
86P23	0.7010	0.1685
92P209	0.4610	0.1695

4.5 Discussion

The results obtained with the Souza-Cardoso dataset suggest that the method proposed can indeed be used to estimate hyperspectral images. As observed in Fig. 4, the estimated reflectance closely follows the true reflectance obtained with a hyperspectral camera. The divergence in the reflectance predicted at higher wavelengths was found to be present on all images analysed. This was confirmed by visual examination of the reconstructed hyperspectral cubes and error computation of the dataset as shown in Fig. 6 where the hyperspectral slice at wavelength 720nm exhibits the highest error. This suggests a potential discrepancy between the acquisition process (e.g. changes in illumination, equipment calibration, data normalisation) of the reference pigment reflectances and the actual hyperspectral data from the images evaluated.

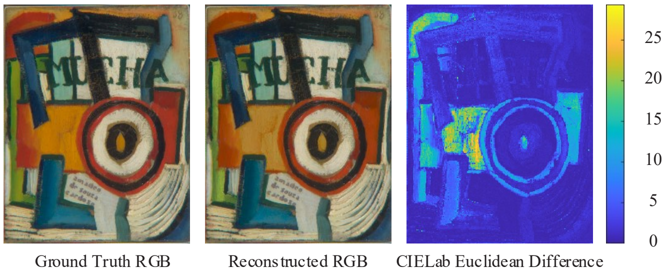

Figure 5: Comparison between RGB version of the ground truth and the reconstructed hyperspectral image of image 86P21. Error map shown as the Euclidean difference of the CIELab colour vectors generated using illuminant D65. ©Center of Modern Art of Calouste Gulbenkian Foundation, Lisbon.

The MRAE values measured between the ground truth and reconstructed images show some variability between all images as this highly penalizes errors. On the other hand, the error measured with SAM shows a more consistent behaviour indicating a good overall reflectance correlation across all images evaluated. This gives an insight into the overall error of the reconstructed reflectances suggesting that while the overall trend of the reconstructed spectra follows the ground truth spectra, there is an error associated with the prediction process. This is thought to be attributed to the lack of base pigments with a higher response at longer wavelengths. The effect can be further exacerbated by other sources of error including differences in the acquisition methods used between the reflectances of the reference pigments and the hyperspectral images of the paintings; while different methods should yield similar reflectance curves, the effect of the illumination and inherent response of the hardware used can result in different reflectances for the same material.

5 CONCLUSION AND FUTURE WORK

Our paper presents a practical method where readily available hyperspectral signatures of reference oil paint pigments are used in conjunction with two DNN structures to reconstruct hyperspectral cubes of paintings, that is when a new unseen RGB image of a painting is provided, a corresponding hyperspectral data can be recovered through such system. The first DNN is trained with the reflectance of artificial colour mixtures and their corresponding colour representation allowing reflectance prediction in the new unseen RGB images. The second DNN serves as a regulator to learn and adjust the inherent characteristics such as illumination and camera properties. Although the results of our method show some errors, in particular at higher wavelengths, the proposed method has achieved promising results for use in the application studied.

The concept of artificial colour mixtures in our study was limited to mixtures of 3 pigment reflectance curves. However, it is recognised that in practice such a mixture rarely is limited in real life; oftentimes the mixture might contain more pigments depending on the style of the artist being studied. This aspect could be also a contributing factor to the errors measured in the case study presented. In other words, the artificial mixture can be generated by any chosen number of pigments with any arbitrary percentages. However, increasing the number of pigments in the mixture and the resolution of their concentrations, results in an increased computational load that grows exponentially potentially rendering the implementation prohibitive.

In conclusion, our approach successfully provides an alternative point of view in terms of spectral reconstruction and is interesting in the art field, when neither hyperspectral cubes of the artworks, nor high-resolution RGB images are easily attainable, yet pre-acquired hyperspectral curves of base materials are available. If the reflectance data of known base pigments is unavailable, the proposed method could be used by building the dictionary of base reflectances from user-selected points of the hyperspectral image of a given painting. Artificial mixtures could then be generated from the selected reflectances thereby allowing to describe other paintings in terms of the chosen data. Thus, to reduce the reconstruction error, a wide selection of points with different colour would be required.

As mentioned previously, the original objective of this work is to compensate for the limited amount of data available for a particular artist, namely hyperspectral information. To follow the current research, a study of the generalisation of the method to explore the generation of hyperspectral data for watercolour paintings and pen drawings is planned. Other work includes the enhancement of the reconstruction method by means of more complex networks and the evaluation of alternative methods for benchmarking.

ACKNOWLEDGMENTS

This work is supported by NOVA LINCS (UIDB/04516/2020) and VICARTE (UIDB/00729/2020), with the financial support of FCT - Fundação para a Ciência e a Tecnologia, through national grant PD/BD/135223/2017.

REFERENCES

[1] Vladimir Afanasiev, A. Ignatenko, and Alexey Voloboy. 2015. The simple method of the rgb to spectrum conversion for tasks of physically based rendering. *Scientific Visualization* 7, 4 (2015), 20–26.

[2] Naveed Akhtar and Ajmal Mian. 2020. Hyperspectral Recovery from RGB Images using Gaussian Processes. *IEEE Transactions on Pattern Analysis and Machine Intelligence* 42, 1 (2020), 100–113. https://doi.org/10.1109/TPAMI.2018.2873729

[3] Boaz Arad and Ohad Ben-Shahar. 2016. Sparse Recovery of Hyperspectral Signal from Natural RGB Images. In *Computer Vision – ECCV 2016*, Bastian Leibe, Jiri Matas, Nicu Sebe, and Max Welling (Eds.). Springer International Publishing, Cham, 19–34.

[4] Jair E. Garcia, Madeline B. Girard, Michael Kasumovic, Phred Petersen, Philip A. Wilksch, and Adrian G. Dyer. 2015. Differentiating Biological Colours with Few and Many Sensors: Spectral Reconstruction with RGB and Hyperspectral Cameras. *PLOS ONE* 10, 5 (may 2015), e0125817. https://doi.org/10.1371/journal.pone.0125817

[5] Rui M. Jesus, Arnaldo J. Abrantes, and Nuno Correia. 2006. Photo Retrieval from Personal Memories Using Generic Concepts. In *Proceedings of the 7th Pacific Rim Conference on Advances in Multimedia Information Processing* (Hangzhou, China) *(PCM'06)*. Springer-Verlag, Berlin, Heidelberg, 633–640. https://doi.org/10.1007/11922162_73

[6] Sriharsha Koundinya, Himanshu Sharma, Manoj Sharma, Avinash Upadhyay, Raunak Manekar, Rudrabha Mukhopadhyay, Abhijit Karmakar, and Santanu Chaudhury. 2018. 2D-3D CNN Based Architectures for Spectral Reconstruction from RGB Images. In *2018 IEEE/CVF Conference on Computer Vision and Pattern Recognition Workshops (CVPRW)*. 957–9577. https://doi.org/10.1109/CVPRW.2018.00129

[7] Paul Kubelka and Franz Munk. 1931. Ein Beitrag zur Optik der Farbanstriche. *Zeitschrift für Technische Physik* 12 (1931), 593–609. Translated to English by

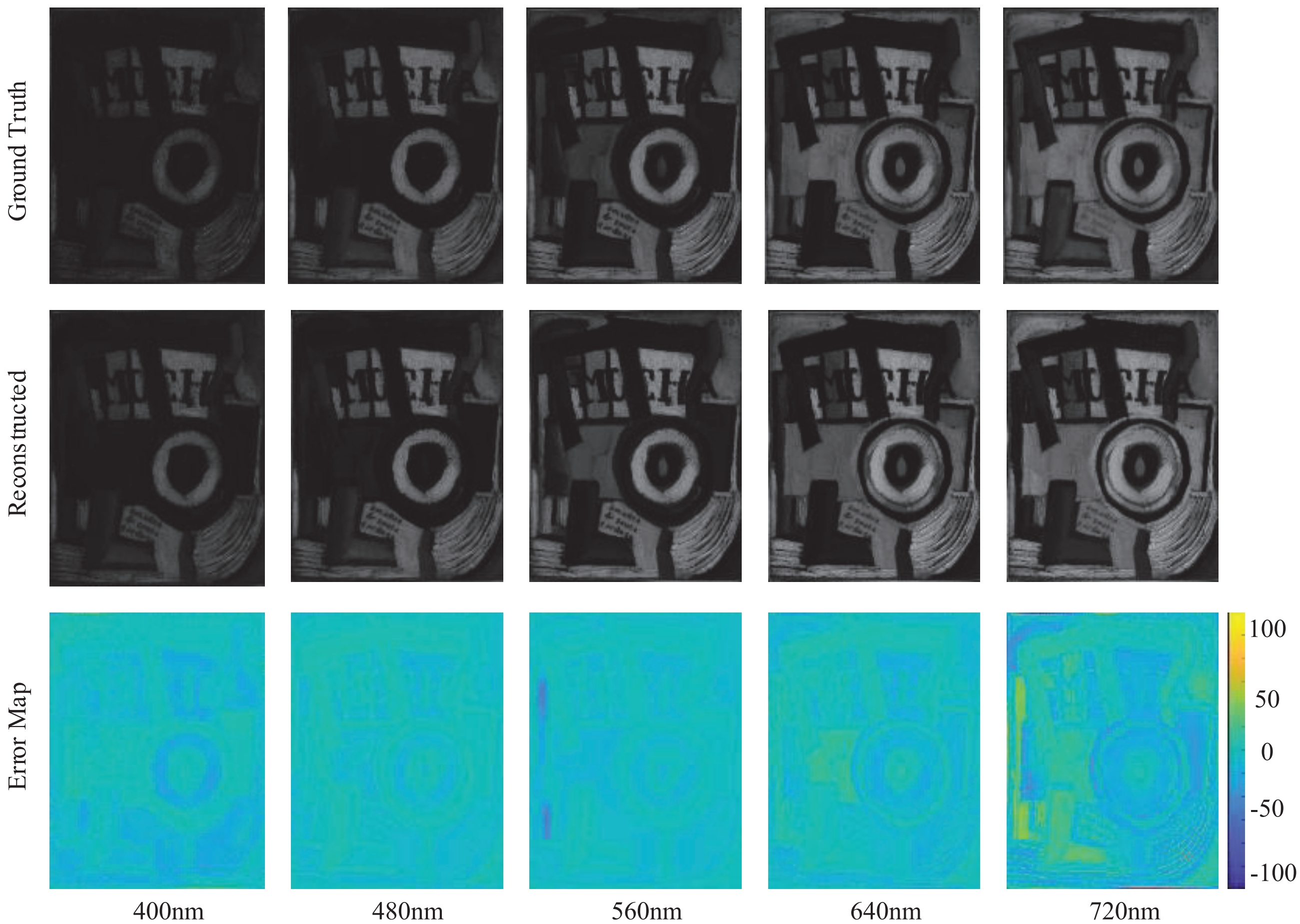

Figure 6: Comparison of reconstructed to ground truth reflectances at selected wavelengths of image 86P21. Error map on a scale of ±255RGB representation of the image used. ©Center of Modern Art of Calouste Gulbenkian Foundation, Lisbon.

Stephen H. Westin, https://www.graphics.cornell.edu/ westin/pubs/kubelka.pdf. 2004.

[8] Cristina Montagner, Rui Jesus, Nuno Correia, Márcia Vilarigues, Rita Macedo, and Maria João Melo. 2016. Features Combination for Art Authentication Studies: Brushstroke and Materials Analysis of Amadeo de Souza-Cardoso. *Multimedia Tools Appl.* 75, 7 (April 2016), 25 pages. https://doi.org/10.1007/s11042-015-3197-x

[9] Seoung Wug Oh, Michael S. Brown, Marc Pollefeys, and Seon Joo Kim. 2016. Do It Yourself Hyperspectral Imaging with Everyday Digital Cameras. In *2016 IEEE Conference on Computer Vision and Pattern Recognition (CVPR)*. 2461–2469. https://doi.org/10.1109/CVPR.2016.270

[10] Zhan Shi, Chang Chen, Zhiwei Xiong, Dong Liu, and Feng Wu. 2018. HSCNN+: Advanced CNN-Based Hyperspectral Recovery from RGB Images. In *2018 IEEE/CVF Conference on Computer Vision and Pattern Recognition Workshops (CVPRW)*. 1052–10528. https://doi.org/10.1109/CVPRW.2018.00139

[11] Lionel Simonot and Mathieu Hébert. 2014. Between additive and subtractive color mixings: intermediate mixing models. *J. Opt. Soc. Am. A* 31, 1 (Jan 2014), 58–66. https://doi.org/10.1364/JOSAA.31.000058

[12] Brian Smits. 1999. An RGB-to-Spectrum Conversion for Reflectances. *J. Graph. Tools* 4, 4 (Dec. 1999), 11–22. https://doi.org/10.1080/10867651.1999.10487511

[13] Longbin Yan, Xiuheng Wang, Min Zhao, Maboud Kaloorazi, Jie Chen, and Susanto Rahardja. 2020. Reconstruction of Hyperspectral Data From RGB Images With Prior Category Information. *IEEE Transactions on Computational Imaging* 6 (2020), 1070–1081. https://doi.org/10.1109/TCI.2020.3000320

[14] Jiangsan Zhao, Dmitry Kechasov, Boris Rewald, Gernot Bodner, Michel Verheul, Nicholas Clarke, and Jihong Liu Clarke. 2020. Deep Learning in Hyperspectral Image Reconstruction from Single RGB images—A Case Study on Tomato Quality Parameters. *Remote Sensing* 12, 19 (2020). https://doi.org/10.3390/rs12193258